

UMTRI-2008-54

NOVEMBER 2008

**INTERSECTION KINEMATICS: A PILOT
STUDY OF DRIVER TURNING BEHAVIOR
WITH APPLICATION TO PEDESTRIAN
OBSCURATION BY A-PILLARS**

MATTHEW P. REED



INTERSECTION KINEMATICS: A PILOT STUDY OF DRIVER
TURNING BEHAVIOR WITH APPLICATION TO PEDESTRIAN
OBSCURATION BY A-PILLARS

Matthew P. Reed

The University of Michigan
Transportation Research Institute
Ann Arbor, Michigan 48109-2150
U.S.A.

Report No. UMTRI-2008-54
November 2008

Technical Report Documentation Page

1. Report No. UMTRI-2008-54	2. Government Accession No.	3. Recipient's Catalog No.	
4. Title and Subtitle Intersection Kinematics: A Pilot Study of Driver Turning Behavior with Application to Pedestrian Obscuration by A-Pillars		5. Report Date November 2008	
		6. Performing Organization Code 302753	
7. Author(s) Reed, M.		8. Performing Organization Report No. UMTRI-2008-54	
9. Performing Organization Name and Address The University of Michigan Transportation Research Institute 2901 Baxter Road Ann Arbor, Michigan 48109-2150 U.S.A.		10. Work Unit no. (TRAIS)	
		11. Contract or Grant No.	
12. Sponsoring Agency Name and Address The University of Michigan Industry Affiliation Program for Human Factors in Transportation Safety		13. Type of Report and Period Covered	
		14. Sponsoring Agency Code	
15. Supplementary Notes The Affiliation Program currently includes Alps Automotive/Alpine Electronics, Autoliv, BMW, Chrysler, Com-Corp Industries, Continental Automotive Systems, Denso, Federal-Mogul, Ford, GE, General Motors, Gentex, Grote Industries, Hella, Hitachi America, Honda, Ichikoh Industries, Koito Manufacturing, Lang-Mekra North America, Magna Donnelly, Mitsubishi Motors, Muth, Nissan, North American Lighting, OSRAM Sylvania, Philips Lighting, Renault, SABIC Innovative Plastics, Sisecam, SL Corporation, Stanley Electric, Toyota Technical Center USA, Truck-Lite, Valeo, Visteon, and 3M Visibility and Insulation Solutions. Information about the Affiliation Program is available at: http://www.umich.edu/~industry/			
16. Abstract Vehicle turn trajectories from a naturalistic driving database were modeled using Bezier curves. A-pillar geometry from 56 vehicles was analyzed to develop representative and extreme cases of A-pillar obscuration. A new methodology was developed for quantifying plan-view obscuration in intersections during left turns. The driver-side A-pillar results in a region of high obscuration immediately to the left of the entrance to the intersection-departure lane. The analysis showed that A-pillars that are closer to the forward line of sight result in high-obscuration regions that are closer to the vehicle travel path. Pedestrians in these regions would be at risk of remaining undetected by a driver. Turn trajectories within the range observed also affected the distribution of obscuration, with shallower turns producing less severe obscuration.			
17. Key Words safety, driver modeling, intersections, vision		18. Distribution Statement Unlimited	
19. Security Classification (of this report) None	20. Security Classification (of this page) None	21. No. of Pages 24	22. Price

ACKNOWLEDGMENTS

Appreciation is extended to the members of the University of Michigan Industry Affiliation Program for Human Factors in Transportation Safety for support of this research. The current members of the Program are:

Alps Automotive/Alpine Electronics	Lang-Mekra North America
Autoliv	Magna Donnelly
BMW	Mitsubishi Motors
Chrysler	Muth
Com-Corp Industries	Nissan
Continental Automotive Systems	North American Lighting
Denso	OSRAM Sylvania
Federal-Mogul	Philips Lighting
Ford	Renault
GE	SABIC Innovative Plastics
General Motors	Sisecam
Gentex	SL Corporation
Grote Industries	Stanley Electric
Hella	Toyota Technical Center, USA
Hitachi America	Truck-Lite
Honda	Valeo
Ichikoh Industries	Visteon
Koito Manufacturing	3M Visibility and Insulation Systems

The authors acknowledge the valuable assistance of Chris Schoeps, Joel Devonshire, and Michelle Barnes of UMTRI.

CONTENTS

ACKNOWLEDGMENTS	ii
INTRODUCTION.....	1
METHOD	2
Intersection Kinematics Data	2
Data Processing	3
<i>Trajectory Interpolation</i>	3
<i>Extracting Turns</i>	4
<i>Bézier Curve Fitting</i>	4
Vehicle Geometry.....	5
Obscuration Simulations.....	7
RESULTS.....	9
Representing Intersection Trajectories Using Bézier Curves	9
Obscuration Analyses	14
DISCUSSION.....	18
Modeling Intersection Trajectories.....	18
Modeling Obscuration	18
Limitations and Further Work.....	19
REFERENCES.....	21

INTRODUCTION

The front pillars on a vehicle's upper body structure, known as A-pillars, support the windshield and roof, but also obstruct the driver's vision of the forward scene. Large vision obscurations due to A-pillars have been linked to increased risk of crashes involving pedestrians during vehicle turning maneuvers. As part of a broader effort to understand the relationship between vehicle geometry and crash risk, this report examines the obscuration of targets in the environment for drivers making right-angle turns at intersections.

A statistical analysis of naturalistic driving data yielded a parametric model of vehicle kinematics during turns based on Bézier splines. Vehicle A-pillar geometry data were obtained from detailed measurements on a convenience sample of 56 passenger cars, minivans, light trucks, and SUVs. The mean A-pillar geometry with respect to driver eye locations and four vehicles representing extremes in the data were used to analyze intersection obscurations.

A computer simulation method was developed to compute pillar obscurations during an intersection turn. The results were analyzed to quantify the effects of turn trajectory and A-pillar geometry within the observed ranges of these variables.

METHOD

Intersection Kinematics Data

The Road Departure Crash Warning (RDCW) study conducted at UMTRI gathered driving data from 87 men and women operating 11 nominally identical passenger sedans (LeBlanc et al. 2007). The drivers used the test vehicle as their own vehicle for four weeks, during which extensive data were gathered on vehicle operations. Relevant to the current study, the data included latitude and longitude from a differential global positioning system (GPS) receiver, longitudinal speed from the vehicle sensor, and steering wheel angle.

Intersections in Washtenaw County, Michigan, were identified using road data from the Highway Performance Monitoring System. These data are generated by local agencies and sent to the Michigan Department of Transportation. The road data were merged with the signalized intersection inventory generated by the Southeast Michigan Council of Governments (SEMCOG) to identify intersections by latitude, longitude, and the names of the roads. The integration was performed using ESRI ArcMap software.

For the current pilot study, vehicle data were extracted for events in which a subject vehicle passed within 100 m of signalized intersections in Washtenaw County. A total of 1138 turns from 87 drivers were identified.

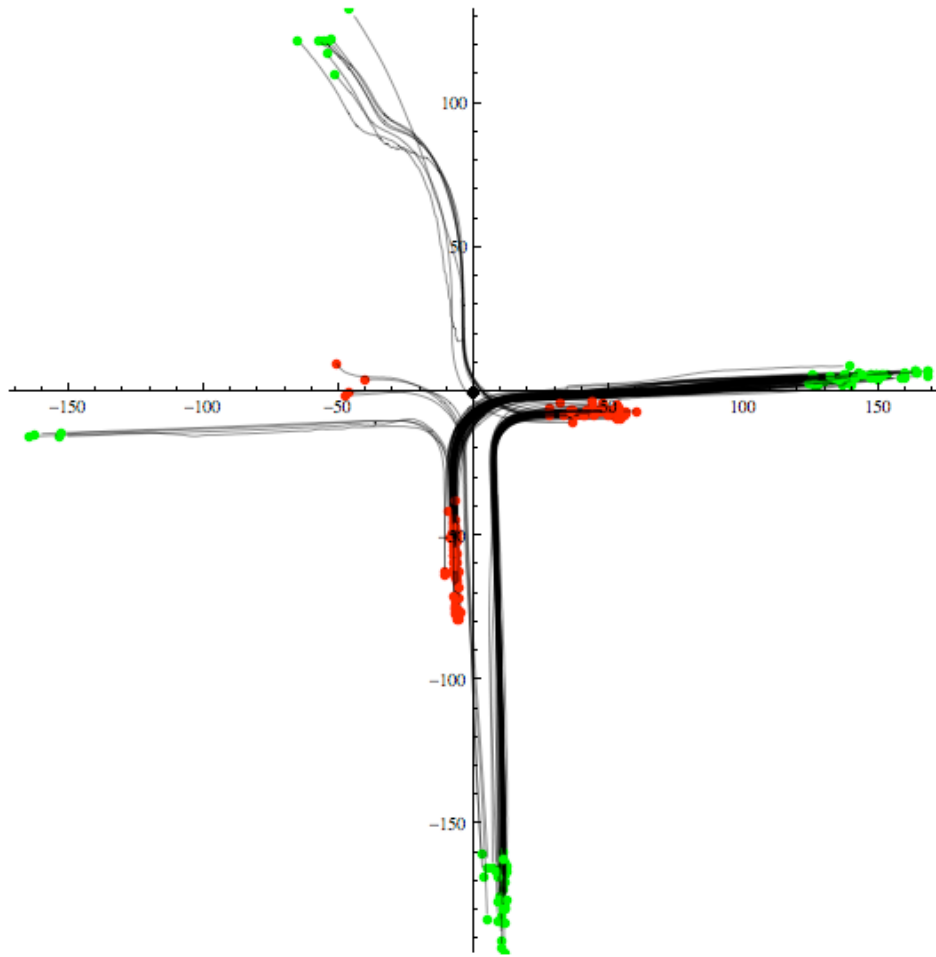


Figure 1. Examples of resampled GPS turn data from the Huron Parkway (vertical road) and Plymouth Road (horizontal) intersection. Green dots indicate the starting point for each trajectory. Dimensions are in meters.

Data Processing

Trajectory Interpolation – The available GPS data exhibited discontinuities in time, with the position remaining constant for several time steps even while the vehicle was in motion. To obtain a smooth trajectory over time, the vehicle speed (from the speedometer signal) was used to resample the spatial trajectory data. An interpolation function was created on both spatial coordinates, relating coordinate value to displacement along the curve. The speed was integrated at each time step to estimate displacement along the trajectory. The overall displacement during the data sample was used to compensate for drift in the integral. The outcome of this step was a smooth displacement trajectory vs. time for all events.

Extracting Turns – Steering wheel angle data were used to extract the portion of each event during which the vehicle was turning. The turn was defined as the time during the event within which the absolute steering wheel angle relative to straight ahead was greater than 10 degrees, plus 0.5 seconds on each end.

Bézier Curve Fitting — One objective of this project was to identify a concise, readily applicable, and computationally simple method for representing distributions of intersection trajectories. Several options were considered, including modeling steering behavior rather than the vehicle trajectory. A Bézier curve description of the vehicle trajectory was ultimately selected as providing good accuracy and a concise set of parameters that are readily calculated and interpreted.

A Bézier curve is a parametric curve in which the positions of the curve can be considered to be a weighted sum of control points. Bézier curves are widely used in computer graphics and drawing programs because their parameterization provides powerful and intuitive control of curvature. Figure 2 shows a third-order (cubic) Bézier curve, the type most commonly used in computer graphics. The curve is defined by four control points, the first and fourth of which are interpolated by the curve. The curve lies fully within the convex hull of its control points. The inner two control points define the curvature, with the gradient at each endpoint defined by the vector from the endpoint to the adjacent control points.

The appeal of the Bézier curve for the current application is that, in general, the end points and the gradients at the end points are known. That is, the orientations of the roads approaching and departing an intersection are known, and points within the approaching and departing lanes can be defined. Moreover, the vehicle will be aligned with the approaching and departing roads at the approaching and departing points, providing a clear interpretation for the P0-P1 and P2-P3 vectors in Figure 2. If the end points and starting and ending gradients are given by the intersection geometry, then the vehicle trajectory can be described by only two parameters, representing the distances P0 to P1 and P2 to P3.

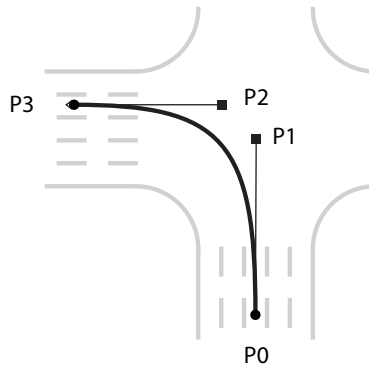


Figure 2. Representation of a left turn trajectory using a Bézier curve.

Bézier curves were fit to the turns extracted from the event data. To avoid a disproportionate weight to samples obtained while the vehicle was stationary (e.g., waiting for a traffic signal) the spatial trajectory data were resampled to 100 evenly spaced points using local second-order polynomial interpolation. Bézier curves that interpolated the end points were computed using linear least-squares methods. The algorithm uses iteration to establish optimal parameter values for each data point while minimizing global error.

Vehicle Geometry

In a separate study, detailed measurements of vehicle interior and exterior geometry were recorded for 56 passenger cars, minivans, SUVs, and light trucks. The data were used to locate the eyellipse according to SAE J941 and to perform pillar obscuration calculations according to SAE J1050. For the current analysis, the left and right A-pillar geometries were located with respect to the centerline of the vehicle and the cyclopean eyellipse centroid. The average values of these variables were used to create the generic vehicle representation shown in Figure 3.

To conduct obstruction simulations, two eye locations at the fore-aft position of the cyclopean centroid separated lateral by 65 mm (the interpupillary breadth used in SAE J941) were used as the origin of rays passing through the right and left A-pillar tangent points, producing a representation of the planar regions obscured to one or both eyes. Note that this approach does not incorporate the head turn and forward eye

positions used in SAE J1050, but provides greater simplicity because the same pair of eye points can be used for varying A-pillar geometries.

A statistical analysis of the A-pillar geometry was used to develop a set of “boundary vehicles” representing extreme combinations of two variables previously shown to be associated with crash risk (Sivak et al. 2006): the angle of the inside edge of the driver-side A-pillar with respect to forward and the angular width of the A-pillar, both measured in plan view with respect to the centroid of the J941 cyclopean eyellipse. A regression analysis was conducted predicting principal component scores of the A-pillar boundary points from these angles. The two angles were only moderately correlated in the data ($r = 0.35$), so a set of four vehicles was constructed using 5th- and 95th-percentile values of the two variables, which were respectively 21.5 and 29.8 degrees for the angle of the pillar with respect to forward and 9.0 and 13.0 degrees for the angular width. The regression analysis gave the mean expected pillar tangent point locations on both the driver and passenger side for these inputs, as shown in Figure 3.

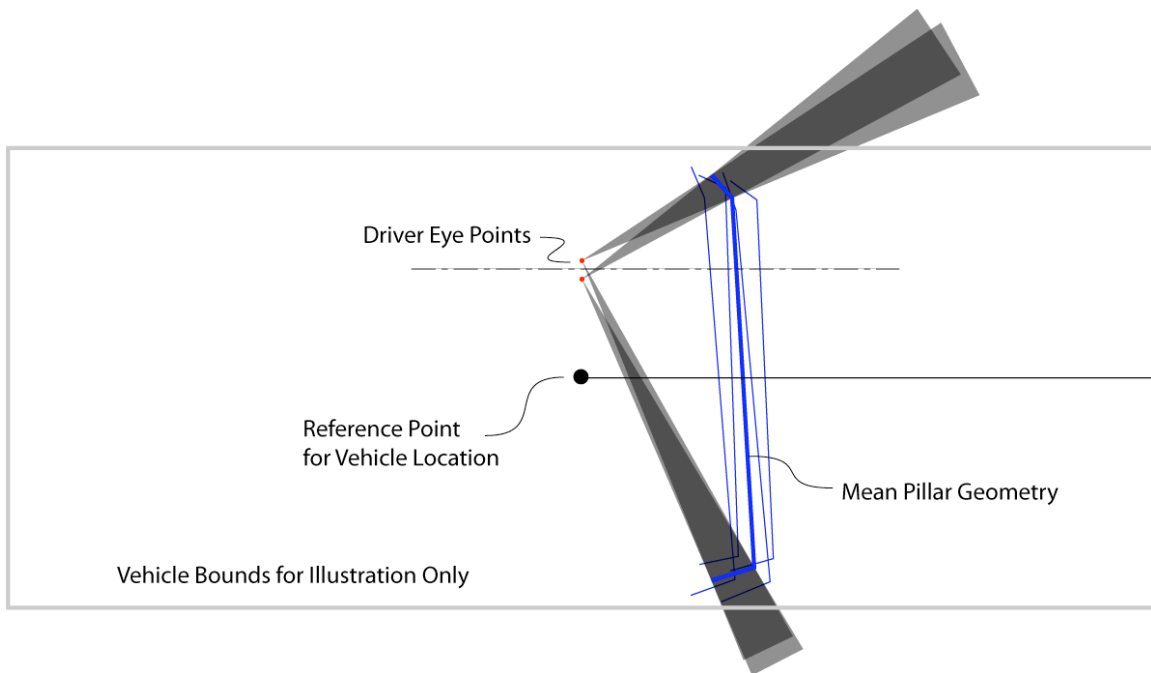


Figure 3. Vehicle and driver geometry used to assess target obscuration. Mean and boundary pillar tangent points are shown, along with obscuration zones for the mean geometry.

Obscuration Simulations

A series of simulations was conducted to assess the effects of turn trajectory on obscuration of locations in the intersection. The mean vehicle shown in Figure 3 was moved along the trajectory in equal displacement increments with the obscuration windows (both eyes, left and right sides) calculated at each increment. Figure 4 shows the 20 positions during one left turn. Raster image calculations were performed to determine the relative amount of the trajectory for which locations in and near the intersection are obscured. At each pixel in the raster, a value of zero was assigned if neither eye was obstructed by the A-pillar, a value of 0.5 indicated obscuration from the location of one eye, and a value of 1.0 indicated obscuration from both eye locations. Figure 5 shows an example raster image, where values of 1.0 are shown in black. The values for each pixel were totaled across the images generated for each position on the trajectory and divided by the number of images to obtain the average obscuration value.

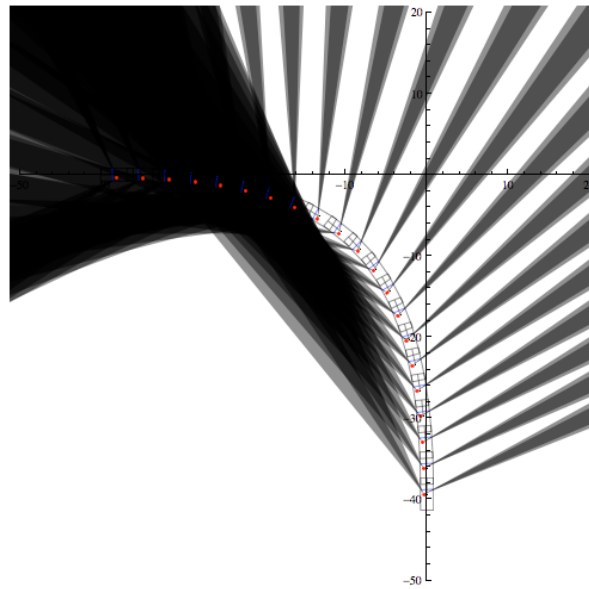


Figure 4. Mapping obscuration at 20 discrete points during a left turn.

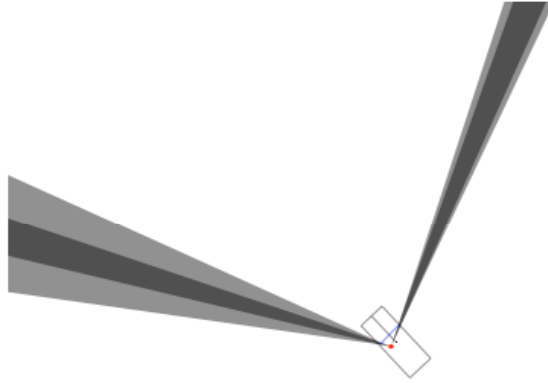


Figure 5. Mapping obscuration in a raster image.

RESULTS

Representing Intersection Trajectories using Bézier Curves

Figure 6 shows examples of intersection trajectories fit using this technique. In general, the Bézier curve was found to fit the trajectories very well. The median root mean squared error value was 0.15 m and 95% of RMS errors were below 0.56 m using 100 evenly spaced sample points on each trajectory.

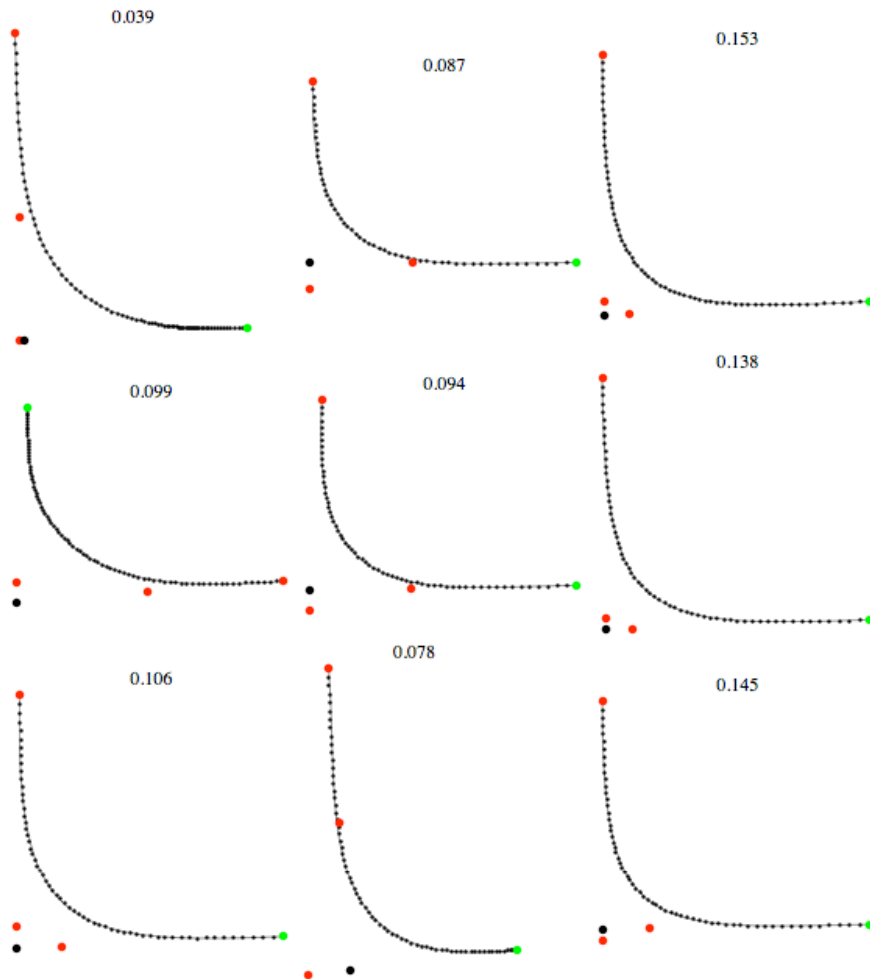


Figure 6. Intersection trajectory data (small dots) fit with Bézier curves (lines). The starting point (green dots) and the interior Bézier control points (red dots) are shown. The black dots show the intersections of the P0-P1 and P3-P4 vectors. The RMS error (meters) for 100 evenly spaced points on the trajectory is listed.

The right and left turns with net orientation change from 80 to 100 degrees, based on the Bézier curve gradients at the beginning and end of the turn trajectory, were extracted for further analysis. In all, 104 left and 127 right turns from a total of 42 subjects were obtained. The median and 95th-percentile RMS errors for the Bézier fits of right-angle turns were 0.11 and 0.26 m, respectively. The right-angle turns included data from 49 subjects with seven subjects accounting for at least 10 turns each. Forty-one of the right-angle turns were recorded at the intersection of Plymouth Road and Huron Parkway, near UMTRI, and four other intersections had at least 10 turns.

The turns were normalized for further analysis. The data were centered at the intersection of the two control vectors (P0-P1 and P3-P4 in Figure 2) and were rotated so that the approach vector was aligned with the Y axis. Control points P3 and P4 were then rotated around the origin to align with the X axis. Given the selection criteria for right-angle turns, these adjustments were 10 degrees or less. Figure 7 shows overlay plots of all right and left normalized turns.

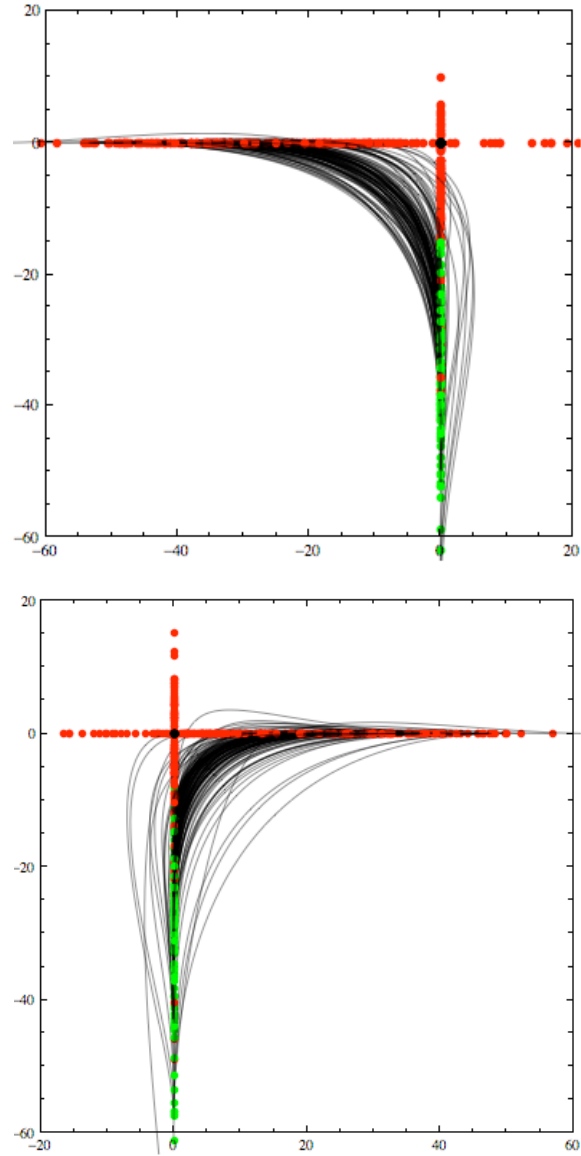


Figure 7. Overlay plots of all normalized left and right turns (meters).

To better visualize the differences in turn shape, the data were further normalized by scaling the trajectories in the plane to set P_0 to $\{-1, 0\}$ and P_4 to $\{-1, 0\}$ or $\{1, 0\}$ for left and right turns, respectively. Figure 8 shows the normalized left and right turns after scaling.

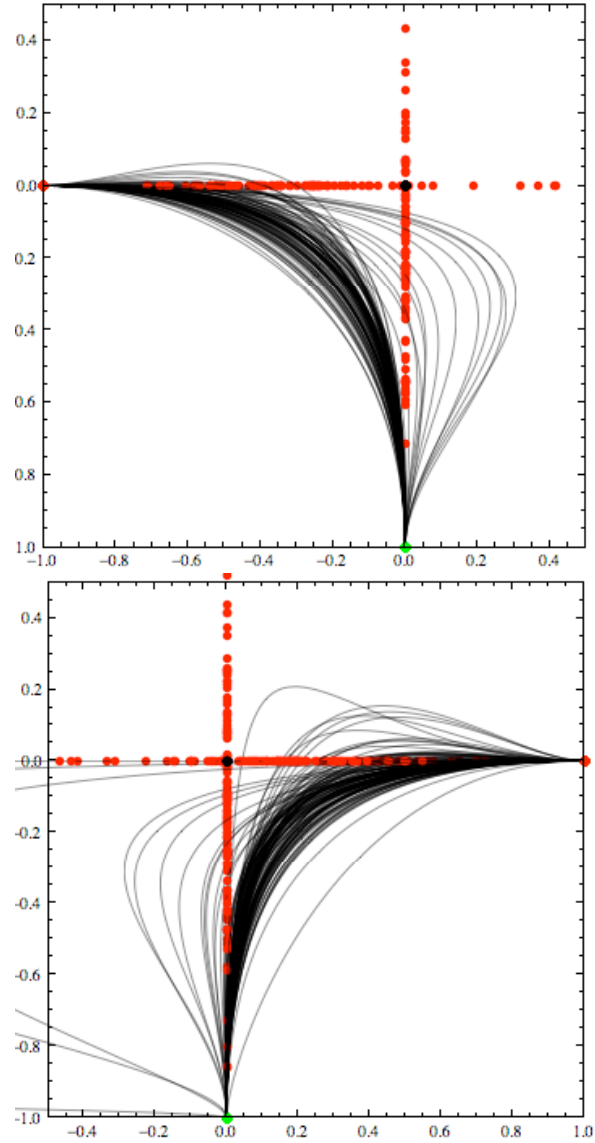


Figure 8. Overlay plots of normalized and scaled left and right turns (dimensionless).

The normalized and scaled turns are each described by only two parameters: the Y coordinate of P2 and the X coordinate of P3 in the scaled coordinate system. Table 1 lists the means and standard deviations of P2 (Y coordinate) and P3 (X coordinate) for left and right turns. The smaller absolute values for the right turns reflect the sharper curvature at the turn apex. The more negative P3X value for left turns, compared with the P2Y value, indicates that left turns are characterized by greater curvature earlier in the turn. The correlation between P2Y and P3X is -0.75 for left turns and 0.57 for right turns. Figure 9 shows the average left and right turns in the scaled space.

Table 1
Means and standard deviations of P2Y and P3X for left and right normalized scaled turns
(dimensionless).

Turn Direction	Parameter	Mean	SD
Left	P2Y	-0.181	0.231
	P3X	-0.256	0.392
Right	P2Y	-0.082	0.307
	P3X	0.109	0.643

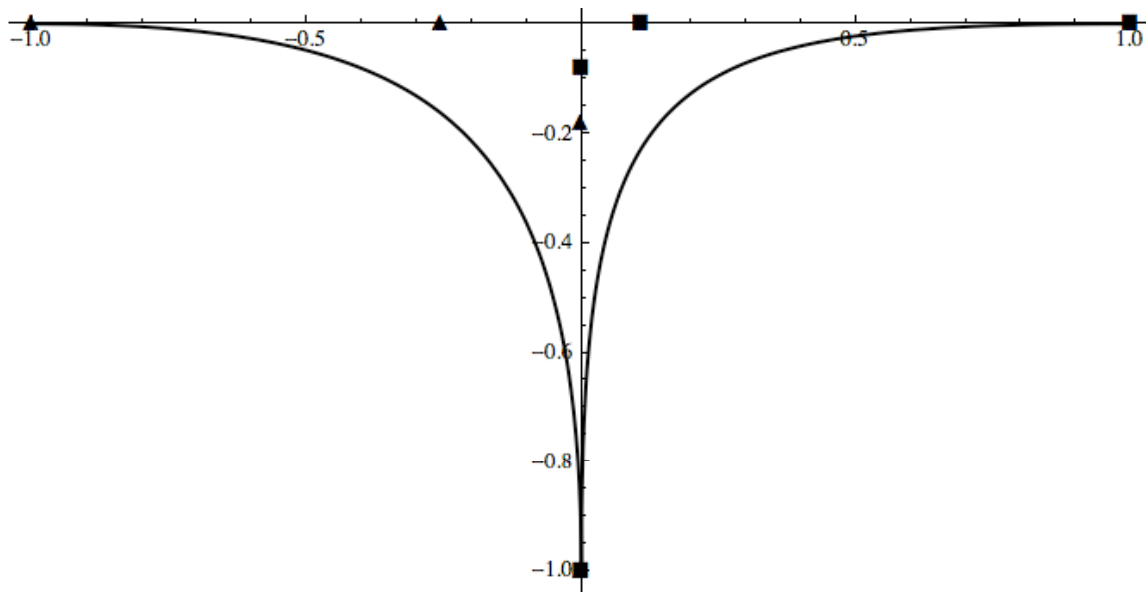


Figure 9. Average left turns (triangle) and right turns (squares) in the scaled space
(dimensionless).

The description of the right-angled turns is completed by the values for P0Y and P4X in the normalized (but not scaled) space. Table 2 gives the means and standard deviations of these values for left and right turns. The correlation between these two parameters is -0.26 for left turns and 0.12 for right turns.

Table 2
Means and standard deviations of P0Y and P4X for left and right normalized turns (meters).

Turn Direction	Parameter	Mean	SD
Left	P0Y	-34.7	11.2
	P4X	-37.5	10.5
Right	P0Y	-29.3	12.0
	P4X	30.1	10.1

Obscuration Analyses

Figure 10 shows the result for the average left turn and mean vehicle geometry. The geometry of an intersection of two five-lane roads is overlaid. The important obscuration is generated by the left A-pillar and is centered in and directly to the left of the target lane. The peak obscuration value was 0.56 at location $\{-18.5, -6\}$ indicating that this point was obscured during 56% of the sampled points on the turn, giving monocular obscuration half as much weight as binocular obscuration. More meaningfully, the centroid point was fully obscured for 61% of sampled points prior to reaching the projected location of the peak obscuration point onto the turn, and obscured for a single eye point for an additional 31%. This indicates that a vision target at this location is at least partially obscured from the simulated eye locations for over 90% of the length of the turn trajectory prior to passing adjacent to the location. The centroid point lies 2.8 m from the vehicle center trajectory at the closest point.

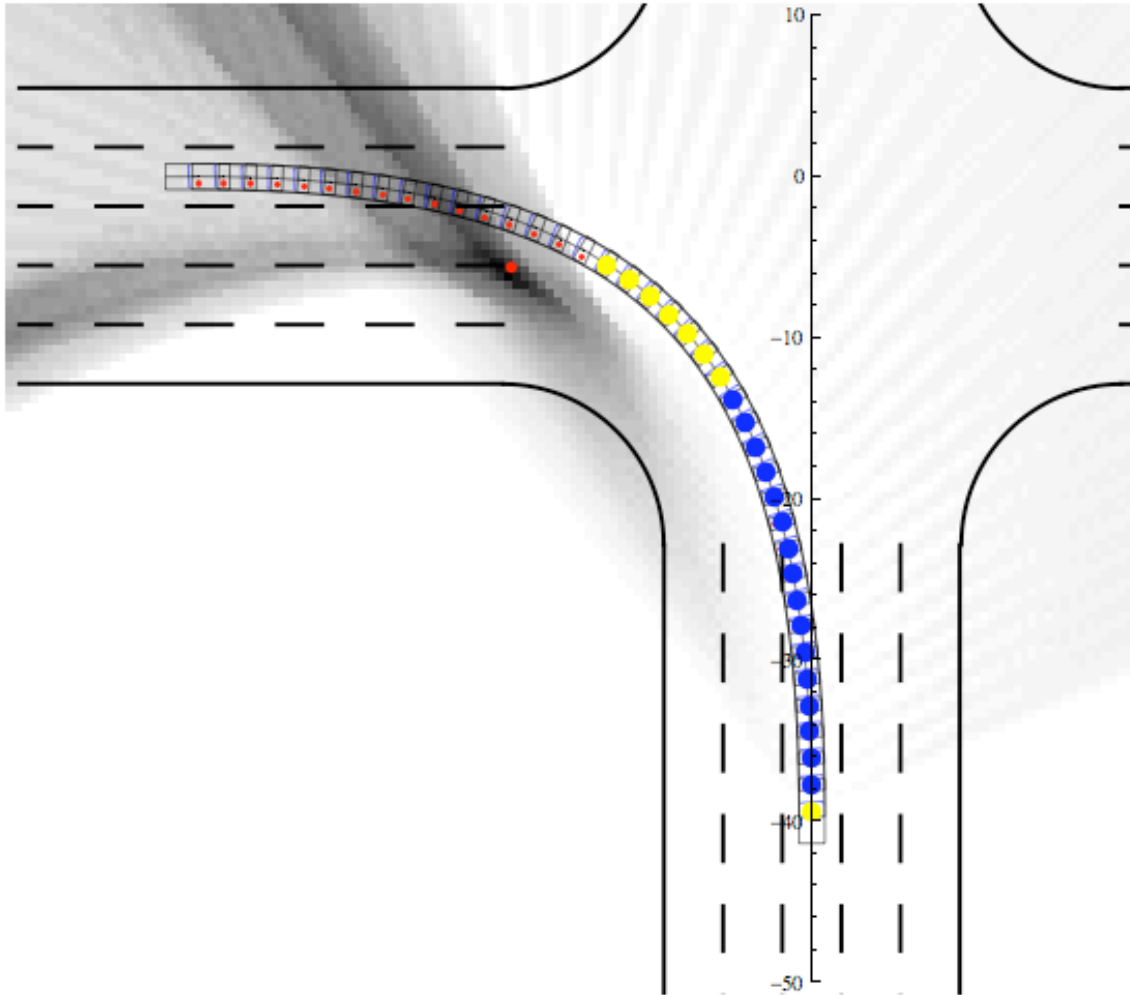


Figure 10. Raster image of obscuration for the average left turn from Plymouth Road to Huron Parkway and the mean vehicle geometry. Darker shading indicates greater fractional obscuration. Obscuration was sampled for 40 evenly spaced points along the trajectory at 0.5 m resolution on the ground plane. The red dot at the centroid of the most obscured zone (obscuration fraction 0.49 and higher) is visible from neither eye position at the blue vehicle locations and from only one eye location at the yellow vehicle locations. The overlaid road geometry is approximate.

The A-pillar size and location affect the distribution of obscuration. Figure 11 shows obscuration calculations for the average left turn at Plymouth Road and Huron Parkway for the four boundary A-pillar geometries. The centroid of the most occluded two-square-meter area is shown, along with the distance of the centroid from the vehicle centerline path. When the inside edge of the A-pillar is closer to the straight-ahead viewing direction, the centroid of the highly obscured region of the intersection moves closer to the vehicle path.

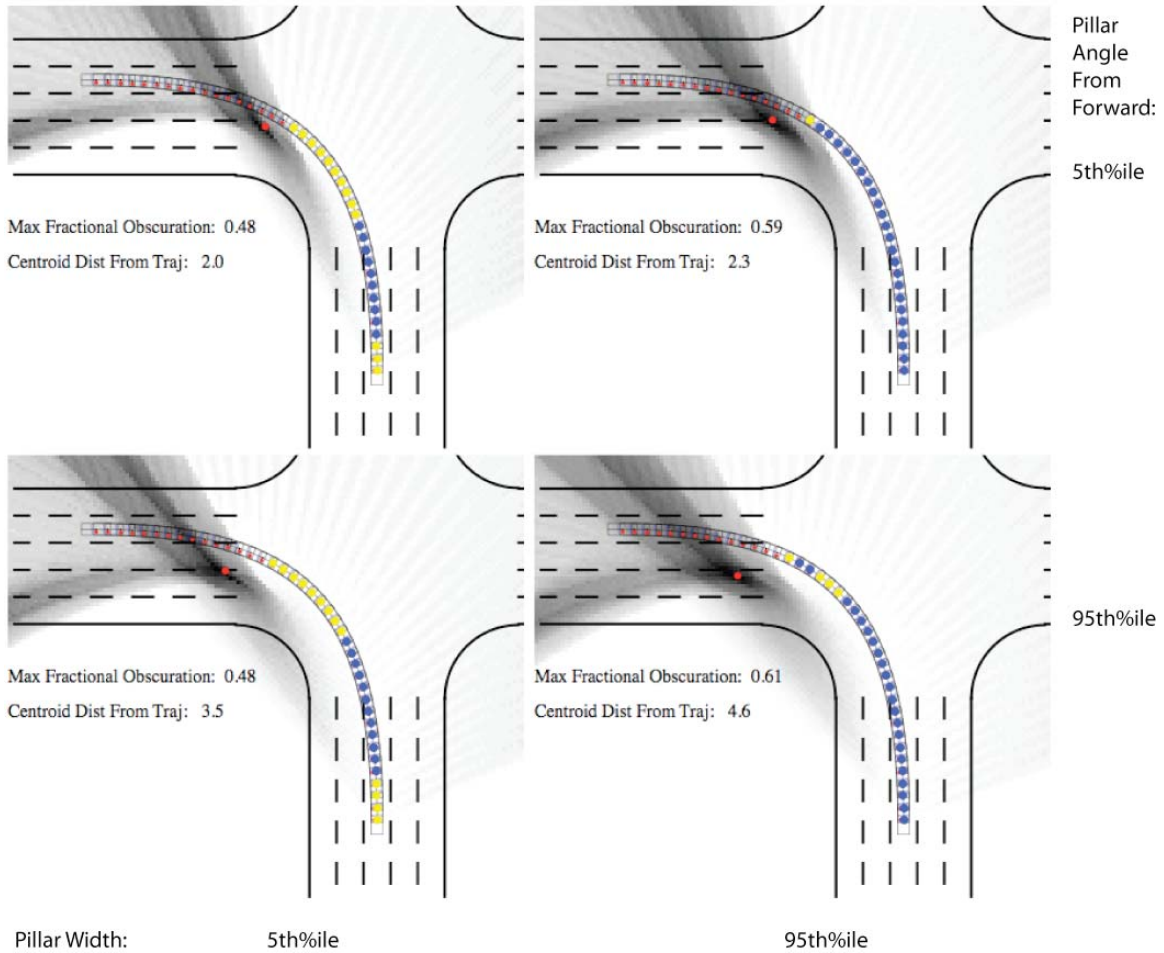


Figure 11. Raster image of obscuration for the average left turn from Plymouth Road to Huron Parkway and vehicle A-pillar geometries representing combinations of 5th and 95th percentiles of driver-side A-pillar angle relative to straight ahead and angular A-pillar width. Darker shading indicates greater fractional obscuration. Obscuration was sampled for 40 evenly spaced points along the trajectory. The red dot at the centroid of the most obscured zone (obscuration fraction 0.4 and higher) is visible from neither eye location at the blue vehicle locations and from only one eye location at the yellow vehicle locations. The overlaid road geometry is approximate.

Vehicle trajectory also affects obscuration. Figure 12 shows obscuration calculations for the mean vehicle geometry and two trajectories computed from the distributions of the normalized, scaled left turns. The turns were constructed from the 5th and 95th percentiles of the first principal component of the normalized, scaled internal control points and the mean end points for left turns. The sharper turn in the left plot of Figure 12 results in a lower peak obscuration, but spreads the obscuration region across the path of the vehicle. The peak obscuration region is usually visible from at least one eye point throughout the turn, but is also moved farther out into the intersection. In contrast, the obscuration region is more concentrated for the more gradual turn on the right of Figure 12 and is farther from the vehicle path.

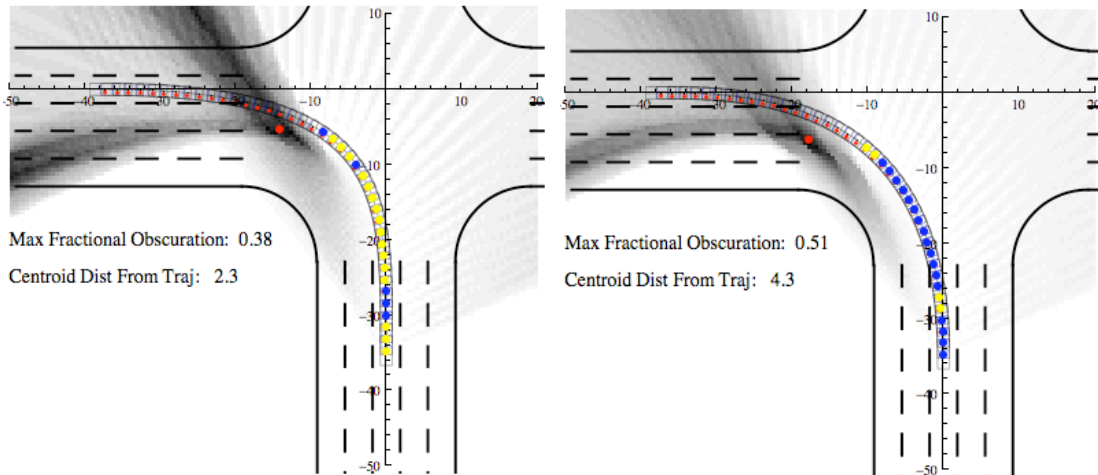


Figure 12. Obscuration maps for the mean vehicle A-pillar geometry and 5th- and 95th percentile left turns based on the distribution of the first principal component of the normalized, scaled left-turn Bézier parameters. See Figure 10 for more information on the plots.

DISCUSSION

Modeling Intersection Trajectories

This report introduced a new method for representing the paths of turning vehicles. The third-order Bézier curve accurately represents the observed vehicle motions with only a small number of parameters. The Bézier parameters are readily interpreted with respect to the gradient at the beginning and end of the turn, providing ready application to simulations of the type undertaken in this work. One relatively arbitrary aspect of the turn definition is the identification of the starting and ending points. In the current work, a steering wheel angle criterion was used. Steering wheel angle is approximately proportional to the yaw rate and hence is more sensitive than an analysis of the vehicle heading. However, drivers often do not immediately move to the center of a lane as they complete a turn, and sometimes drift across lanes as they begin a turn. Nonetheless, the concise description of vehicle trajectory given by the Bézier approach provides a basis for modeling distributions of turning behavior.

Modeling Obscuration

The obscuration assessment methodology presented here combines the effects of A-pillar obscuration and vehicle kinematics to create a map of the relative obscuration of points in the environment. The raster-based approach is computationally efficient compared to other potential approaches for determining whether a sample point is obscured and is easily scaled to a finer grid or a larger number of sampled vehicle points.

The analysis showed that geometry of the A-pillar, over the range observed in vehicles, has a substantial effect on the size and position of the most obscured regions of the intersection relative to the vehicle trajectory. For left turns, the most highly obscured zone is immediately to the left of the vehicle path at the entrance to the intersection-departure lane. In a typical turn, a pedestrian standing at this location would not be visible from the normal driver eye locations for a substantial percentage of the turn. With larger pillars, the size of the zone at a given level of obscuration is increased, but the most important effect was observed when the pillar was moved closer to the forward line

of sight. The region of greatest obscuration moved closer to the vehicle trajectory, potentially creating a greater risk for pedestrians.

Limitations and Further Work

This pilot study introduced new methods for examining vehicle turn trajectories and the effects of A-pillar geometry on obscuration in intersections. Yet, the nature of the underlying data and the analysis methods create some important limitations. The analysis does not consider the temporal aspect of turning. Vehicle speeds varied widely in the dataset, depending on turn radius, traffic density, and other factors. Future work should consider vehicle speeds, in particular to determine the time drivers have to detect and react to pedestrians in or near the vehicle path.

The analysis does not consider the possibility that A-pillar geometry might affect turning trajectories. For example, a driver of a vehicle with larger A-pillar obscurations might tend to use a different turning strategy. The current analysis used turning data from a single vehicle type across multiple drivers and intersections to examine the effects of A-pillar geometry, but the possibility of a vehicle geometry effect on trajectory should be examined.

The obscuration analysis uses two nominal eye locations oriented for straight-ahead viewing. In reality, drivers tend to turn their heads in the direction of the turn. More importantly, drivers tend to move their heads from side to side to view the area behind the pillar. Observations of drivers at intersections have revealed a typical “head bob” in which the driver shifts his or her gaze from looking out of the windshield to looking out the side glass during the early part of the turn, then shifts back to the windshield as the turn is completed. Future work should examine the kinematics and timing of these maneuvers, as well as their effectiveness, because this behavior may substantially ameliorate the issues identified in the current analysis with static eye locations. The fact that many drivers show this pattern of head movement does not obviate the obscuration analysis, however, because drivers may be more or less effective in performing this maneuver due to, for example, reduced cervical spine mobility or distraction.

The obscuration calculations assumed that viewing with one eye yielded 50% of the value of viewing with two eyes. Arguments could be made for both larger and

smaller values. Perhaps a more important consideration is the three-dimensional nature of the target. The current planar analysis neglects the fact that A-pillars are usually angled relative to the driver, so that the obscuration varies with the orientation of the view plane. Conceptually, a tall thin target is more likely to be seen behind an angled pillar than the planar analysis would suggest. However, partial occlusion of a standing pedestrian might greatly reduce the likelihood of detection, suggesting that the planar analysis might be conservative. A deeper understanding of how partial occlusion affects the pedestrian detection task is needed.

REFERENCES

- LeBlanc, D., Sayer, J., Winkler, C., Ervin, R., Bogard, S., Devonshire, J., Mefford, M., Hagan, M., Bareket, Z., Goodsell, R., and Gordon, T. (2007). *Road Departure Crash Warning System Field Operational Test: Methodology and Results* (Technical Report No. UMTRI-2006-9-1). Ann Arbor: The University of Michigan Transportation Research Institute.
- Sivak, M., Schoettle, B., Reed, M.P., Flannagan, M.J. (2006). Influence of visibility out of the vehicle cabin on lane-change crashes. *Accident Analysis and Prevention*, 38, 969-972.